SUPPLEMENTARY INFORMATION

Structural and kinetic basis for the regulation and potentiation of Hsp104 function

Xiang Ye[1,2], JiaBei Lin[2], Leland Mayne[1,2], James Shorter[2], and S. Walter Englander[1,2]

[1]Johnson Research Foundation, [2]Department of Biochemistry and Biophysics, Perelman School of Medicine, University of Pennsylvania, Philadelphia, PA, USA.

Materials and Methods

Protein Purification. WT and mutant proteins were expressed and purified as described (1-3).

Continuous labeling HX MS experiments. Hsp104 was dialyzed into H_2O-buffer (20 mM HEPES, 10 mM $MgCl_2$, 150 mM KCl, 2 mM TCEP (tris(2-carboxyethyl)phosphine), at pH 7.45). D_2O buffer used for D-labeling contained the same components, with pD (pH meter read + 0.4) adjusted to read pD 7.85 (pH + 0.4) after 9 to 1 mixing with protein in H_2O-buffer. To prepare for a typical HX experiment, 20 µM Hsp104 (in [monomer]) was incubated under the desired buffer conditions at 25°C for at least 5 min before H to D labeling. Protein with ATPγS was pre-incubated for 1 hr to allow its slow structure change to reach equilibrium.

H to D labeling was initiated by 10-fold dilution into the corresponding D_2O buffer. HX time points shorter than 10 s were collected by using a Biologic SFM4 stopped-flow device to achieve rapid labeling and quenching, as in(4). After varying HX labeling time, the labeling reaction was quenched by addition of ice-cold quench buffer of equal volume to reach a pH 2.50 and 1.5 M GdmCl and immediately injected into the online analysis system (pepsin digestion, LC separation, and MS measurement as described previously (4-7).

Unless otherwise indicated, ADP and ATP were at 5 mM concentration in both H_2O buffer and D_2O buffer. Under such conditions, it has been shown Hsp104 is predominantly in the hexameric state (8). For experiments under ATP turnover conditions, solutions also contained an ATP regenerating system (20 mM phosphoenolpyruvate and 20 unit/ml pyruvate kinase). For experiments in the presence of substrate protein, denatured carboxymethylated α-lactalbumin from bovine milk was prepared as described in(9). α-lactalbumin was added to H_2O-buffer to 3 fold over Hsp104 hexamer.

ADP binding kinetics. Hsp104 at 20 µM was initially equilibrated with 500 µM ADP for at least 5 min at 25 °C. To initiate ADP dissociation and H to D labeling, the Hsp104-ADP solution was diluted by 10-fold into D_2O labeling buffer containing no ADP at pD 8.35 in a four-syringe Biologic stopped-flow device (20 mM Tricine at pH 8.35 to make D-labeling faster than ADP rebinding, 10 mM $MgCl_2$, 150 mM KCl, and 2mM TCEP). After varying times, the reaction was quenched and samples subsequently processed in the same way as for continuous labeling experiments.

To measure the equilibrium ADP binding constant, varying concentrations of ADP were first incubated with Hsp104, then diluted into the D-labeling buffer and allowed to label for only 40 ms before quenching and analysis to measure the fraction of Hsp104 binding sites occupied by ADP before any significant dissociation occurs.

HX MS data analysis. We used ExMS2 software to identify and analyze deuterated peptides as described in(10). Thanks to the high mass accuracy and scan stability of the mass spectrometer (Q-Exactive orbitrap), we were able to set the narrow mass tolerance range of 2 ppm in assigning m/z peaks to a given peptide. This is critical to reduce false peptide identifications which could be a serious problem for large proteins such as Hsp104 that can generate more than one peptide with similar m/z. Peptides that passed multiple ExMS2 identification check criteria were subject to further manual inspection. Only peptides found in most of the data points, with good signal to noise, no spurious m/z peaks, and consistency with overlapping peptides were included for subsequent analysis.

Steady-state ATP hydrolysis. Steady-state hydrolysis of ATP by Hsp104 was measured by a coupled NADH enzyme assay (11) (Supplementary Fig. 1). The assay was performed under the same buffer condition as in the ADP binding kinetic measurements (20 mM Tricine (pH=8.35), 10 mM $MgCl_2$, 150 mM KCl, 2 mM TCEP) in addition to 5 mM phosphoenolpyruvate (PEP), 20 unit/ml pyruvate kinase, 1mM nicotinamide adenine dinucleotide (NADH), 20 unit/ml lactate dehydrogenase, plus ATP of varying concentrations between 50 μM and 10 mM, 25°C. To initiate the measurement Hsp104 was added to a final concentration of 2 μM. The rate of absorbance decrease at 340 nm was followed in a quartz cuvette with 0.2 cm light path for several minutes and converted to ATP hydrolysis rate (v) by the following equation.

$$v = \frac{\Delta absorption/\Delta time}{6.22 mM^{-1} cm^{-1} * 0.2 cm}$$

in which $6.22 mM^{-1}cm^{-1}$ is the extinction coefficient of NADH at 340nm. The rate (v) was plotted as a function of ATP concentration and fit to the Hill equation, where h is the Hill coefficient.

$$v = k_{cat} \frac{[ATP]^h}{[ATP]^h + K_m}$$

Substrate processing measured by TMR-α-lactalbumin and FITC-casein.

Reduced carboxymethylated α-lactalbumin doubly labeled with tetramethyl-rhodamine (TMR) was prepared using a modified protocol of Kuwajima et al.(12). To selectively reduce the weakest disulfide bond formed between Cys 6 and Cys 120, 100 μM α-lactalbumin in 50 mM HEPES and 1 mM $CaCl_2$ at pH 7 was treated with 3 mM DTT for 2 min at 25°C. DTT was rapidly removed by gel-filtration using a G25 resin packed spin column and 1mM TMR-5-maleimide was added immediately afterward to label the two reduced Cys for 60min at 25°C. Excess DTT and iodoacetate were then added to reduce and fully carboxymethylate the rest of the Cys residues as in(9). The labeling efficiency was measured in terms of the abundance of protein chemical conjugates of different masses in a Q-Exactive orbitrap mass spectrometer. The doubly labeled α-lactalbumin is approximately 80% with a small population of unlabeled and singly labeled species.

Real time fluorescence measurement was performed with an AVIV CD/Fl spectrometer. TMR fluorescence was excited at 555 nm. A 575 nm cutoff filter was used to integrate photons beyond this wavelength. 4 μM Hsp104 protomer was incubated with 300 nM α-lactalbumin/TMR (20 mM HEPES, 10 mM $MgCl_2$, 150 mM KCl, 2 mM TCEP, pH=7.45) for at least 5 min before measurements. The measurement was initiated by addition of 10 mM ATP and an ATP regenerating system with 100 unit/ml

of pyruvate kinase and 5 mM phosphoenolpyruvate. Background fluorescence intensity for Hsp104 and α-lactalbumin/TMR in the absence of nucleotide was subtracted from all the fluorescence traces, and the fluorescence traces obtained in the presence of ATP were normalized to the high value obtained in the presence of 5 mM ATPγS.

Fluorescein isothiocyanate labeled casein (FITC-casein) was purchased from Sigma-Aldrich. Fluorescence anisotropy measurements were performed in a TECAN-infinite M1000 plate reader. The measurements were performed using 100nM FITC-casein under the same buffer conditions as in TMR-αLA measurements except for 10mM instead of 5mM phosphoenolpyruvate was used.

Kinetic parameters for ADP binding to NBD2. A common set of parameters including ADP on/off rates and site-resolved HX rates was used to fit the data collected under the five different conditions shown in Supplementary Fig. 5 plus the apo-state. The process of H to D exchange on the peptide level was modeled by, first of all, defining the kinetic species $H_{<n1, n2, \dots, np>}D_{<m1, m2, \dots, mq>}$, in which $<n_i>$ and $<m_j>$ are indices of exchangeable sites on the peptide in question. These exchangeable sites are either in *H* or *D*. $p+q$ is the total number of exchangeable sites, e.g. for the peptide 612-623, $p+q=10$ (the N-terminal and n+1 residues are not measured). For each exchangeable site, there are two possible exchange rates, i.e. with or without ADP bound. The without ADP bound rate equals that of the apo-state and different

$$H_{<n1, n2, \dots, np>}D_{<m1, m2, \dots, mq>} + \text{ADP} \underset{k_{off}}{\overset{k_{on}}{\rightleftharpoons}} H_{<n1, n2, \dots, np>}D_{<m1, m2, \dots, mq>} \cdot \text{ADP}$$

$$\downarrow kex_{n1} \qquad\qquad \downarrow \varepsilon * kex_{n1}$$

$$H_{<n2, n3, \dots, n(p-1)>}D_{<n1, m1, m2, \dots, m(q+1)>} + \text{ADP} \underset{k_{off}}{\overset{k_{on}}{\rightleftharpoons}} H_{<n2, n3, \dots, n(p-1)>}D_{<n1, m1, m2, \dots, m(q+1)>} \cdot \text{ADP}$$

exchangeable sites may have different HX rates that are optimized by a least-squares based optimization routine (Matlab function *lsqnonlin*). The ADP-bound HX rate is slowed uniformly by a parameter (ε) optimized at the same time. The kinetic species $H_{<n1, n2, \dots, np>}D_{<m1, m2, \dots, mq>}$ with Σm_p deuterons can be converted to a peptide with Σm_p+1 deuterons by replacing any one of the *p* H sites with the site-specific HX rate kex_l, in which $l \in [n_1, n_2, \dots, n_p, m_1, m_2, \dots, m_q]$. For example, if H at the n_1 site is replaced with D, then the following kinetic scheme can be used to describe this exchange event:

The exchange of *H* at sites other than n_1 involves the corresponding kex_l and can be described in the same way. HX of all the possible kinetic species can be conveniently gathered into a system matrix of the following form.

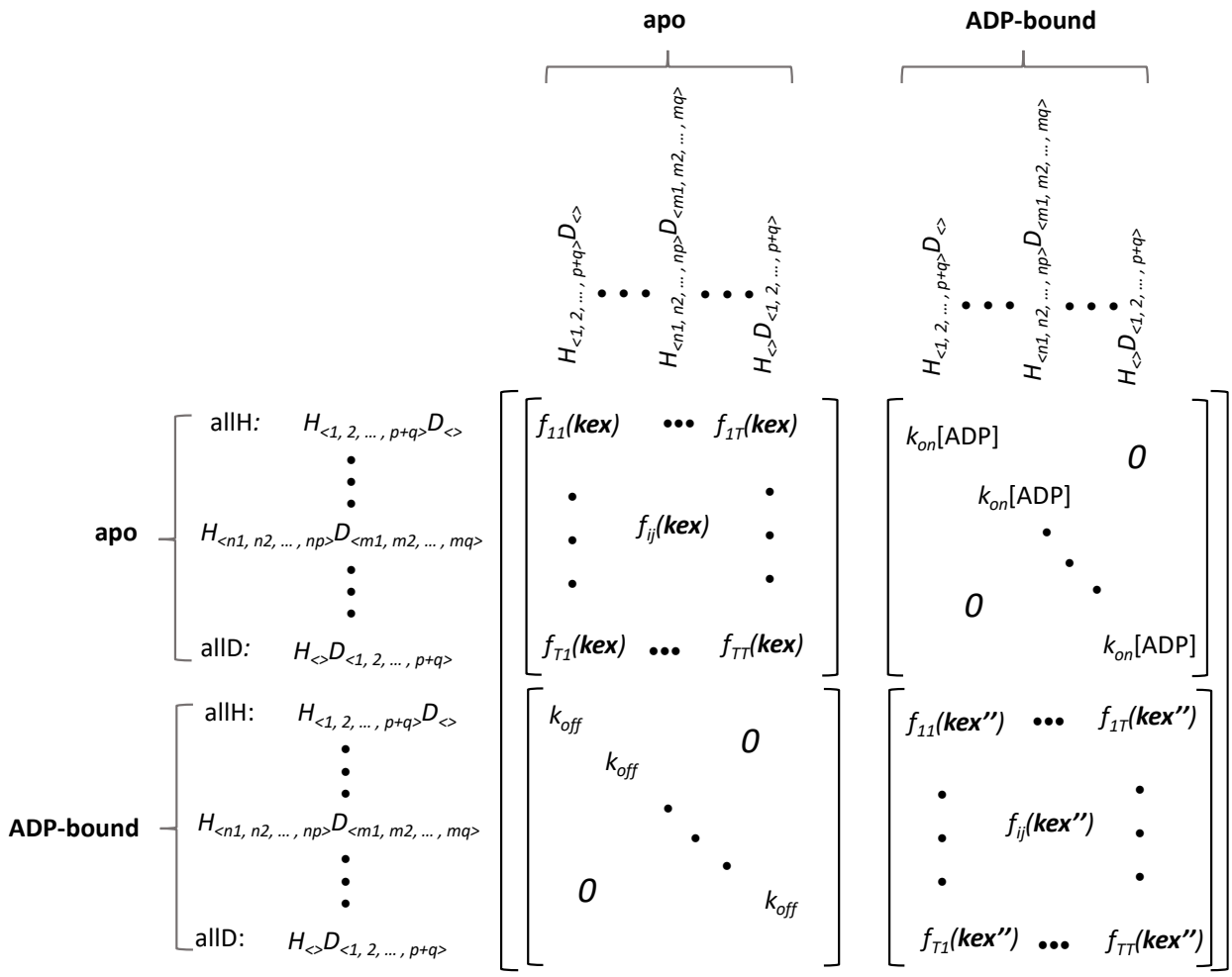

The whole matrix can be divided into four sub-matrices. Each is a square matrix of *T* by *T* dimension, in which $T = 2^{p+q}$ (total number of unique kinetic species). The right upper sub-matrix and the left lower one represent ADP binding and dissociation events. Because ADP on and off does not result in HX, there are only diagonal elements for these sub-matrices. The left upper corner and the right lower corner represent HX events regarding apo or ADP-bound kinetic species. The two sub-matrices are almost identical but for the exchange rate used as previously discussed, i.e. $\boldsymbol{kex'' = \varepsilon * kex}$. $f_{ij}(\boldsymbol{kex})$ is a function of the HX rate vector $kex=[kex_1,\ldots,kex_i,\ldots,kex_{p+q}]$ and summarizes the total influx and efflux of the *i*th kinetic species originating from the *j*th kinetic species. For example, $f_{11}(\boldsymbol{kex}) = -[H_{<n1,n2,\ldots,np>}D_{<m1,m2,\ldots,mq>}] \cdot \sum_{i=1}^{p+q} kex_i$ because all $p+q$ sites can undergo *H* to *D* exchange and results in reduction or efflux of the given kinetic species. On the other hand, $f_{(p+q)(p+q)}(\boldsymbol{kex}) = 0$, i.e. there is no efflux originating from the all D peptide. In the end, the columns of these two sub-matrices should sum to zero, i.e. $\sum_{i=1}^{p+q} f_{ij}(\boldsymbol{kex}) = 0$.

This system matrix (***M***) maps out the pairwise connection between all the different kinetic species and is used to construct the ordinary differential equation group to model HX and ADP on and off simultaneously.

$$d\boldsymbol{P}/_{dt} = \boldsymbol{M} \cdot \boldsymbol{P}$$

in which ***P=***

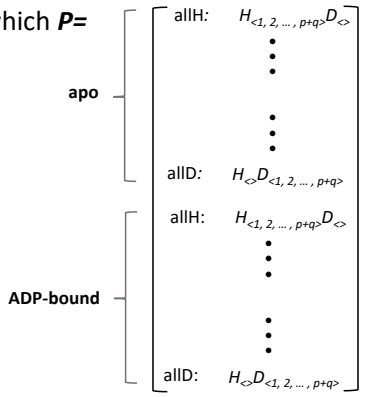

The differential equations are solved numerically by using Matlab function *ode15s* and the resulting D distribution is compared with the experimentally observed one based on the MS spectra. The difference is minimized by adjusting the value of ADP on and off rates (k_{on} and k_{off}), site-revolved HX rates (***kex***), and the uniform slowing factor due to ADP binding (ε). The optimization routine is achieved by using the Matlab function *lsqnonlin*.

Supplementary Figures

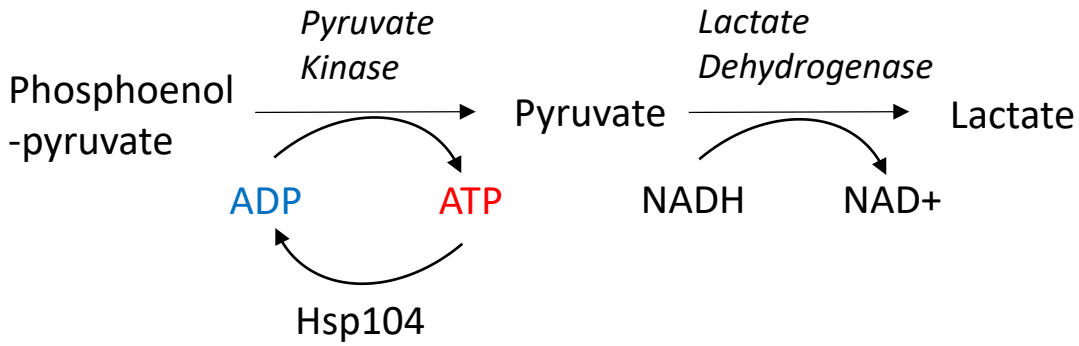

Fig. SI 1. The regenerating coupled enzyme system used to measure ATP hydrolysis by Hsp104 (11). The composition of the system is described in Methods.

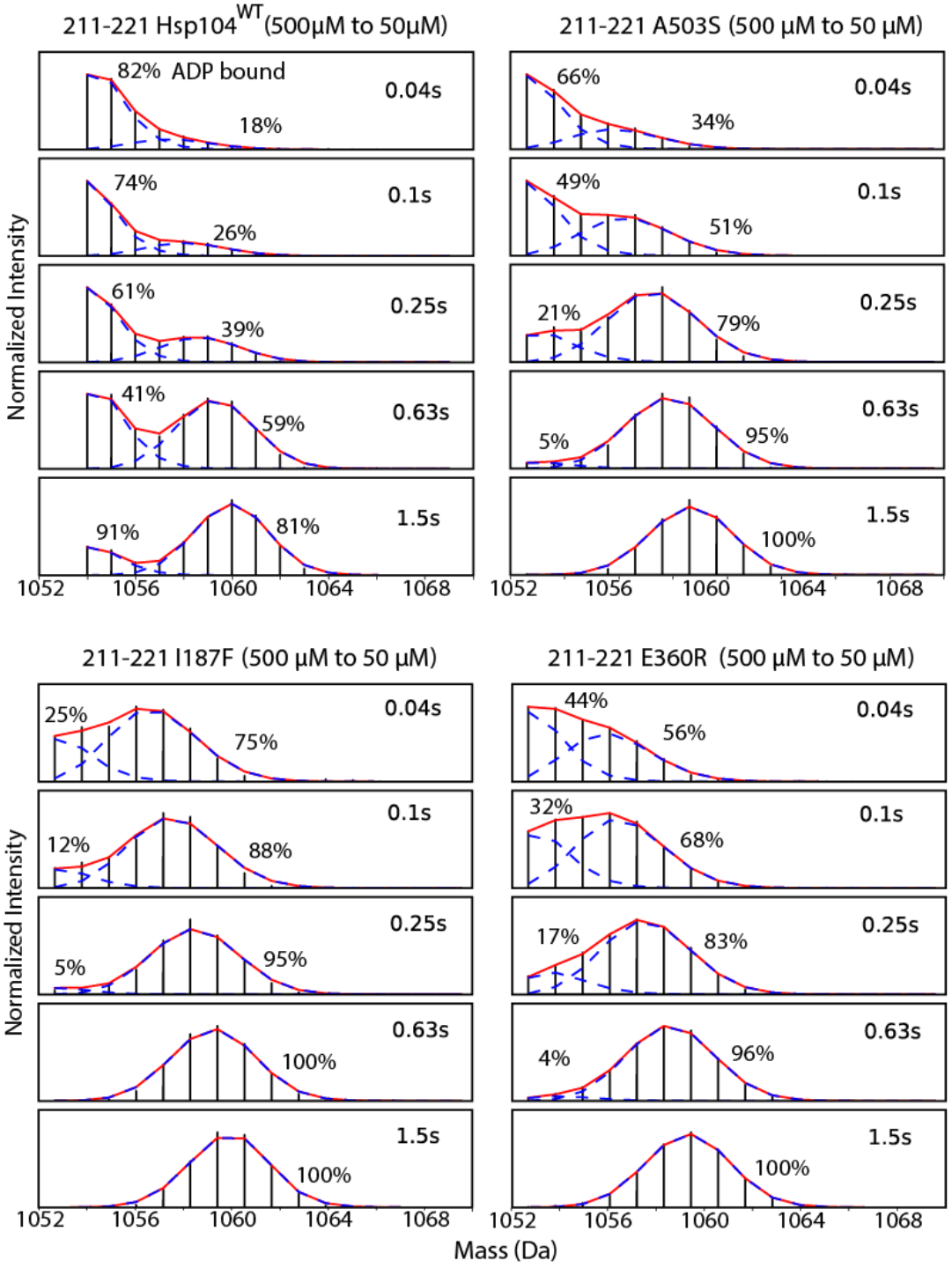

Fig. SI 2. HX MS spectra of the Walker A segment show that potentiated mutants accelerate ADP dissociation from NBD1. The two isotopic envelopes represent the still ADP-bound HX protected population (lighter) and the increasing fraction that has experienced ADP dissociation and D-labeling (heavier). The progression to increasing D-labeling shows the time course for ADP release by WT and the three potentiated mutational variants following dilution from high to low ADP concentrations (as in Fig. 2E).

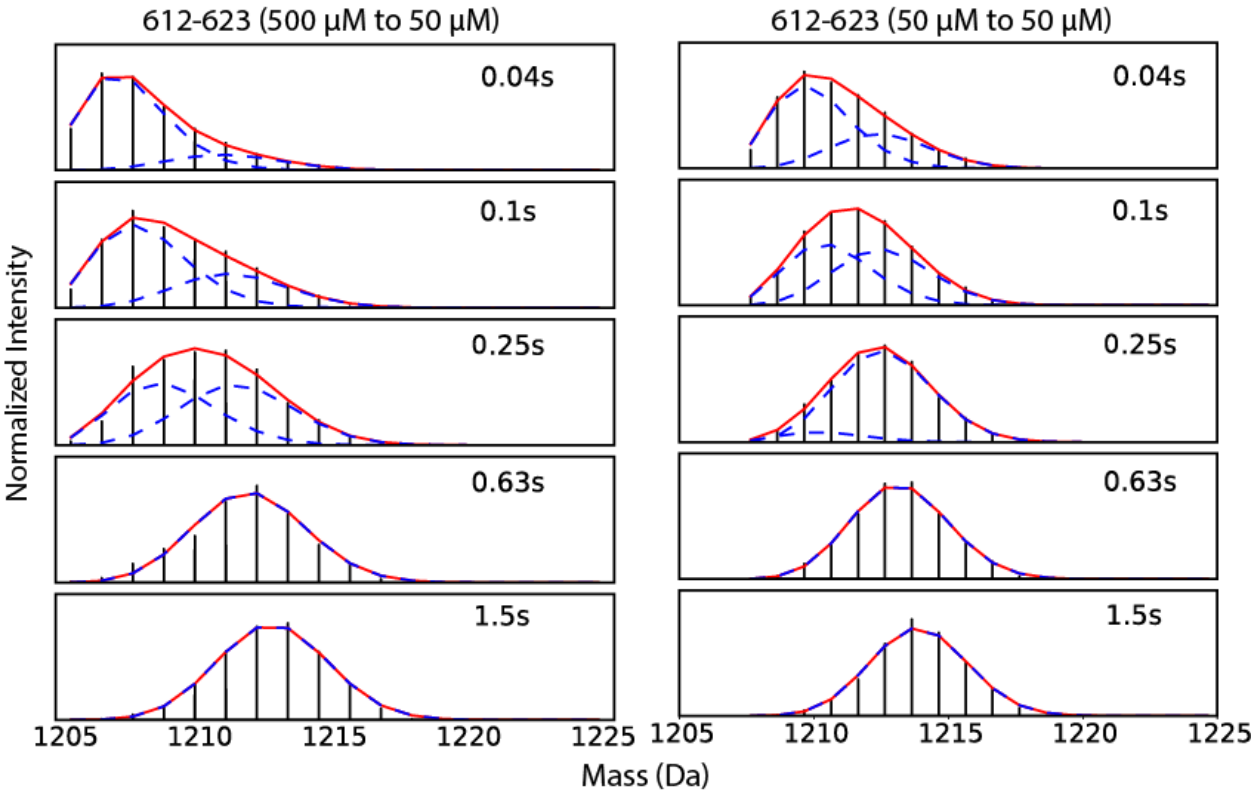

Fig. SI 3. HX MS spectra of the Walker A segment in WT NBD2 shows that ADP binding and dissociation kinetics are much faster than in NBD1. Unlike NBD1, ADP rebinding rate is similar to HX, leading to poor envelope separation. Therefore, the ADP off rate is poorly defined. The MS spectra are sensitive to the different initial ADP concentrations, indicating ADP binding kinetics can be extracted from this kind of experiment as detailed in Supplementary Methods.

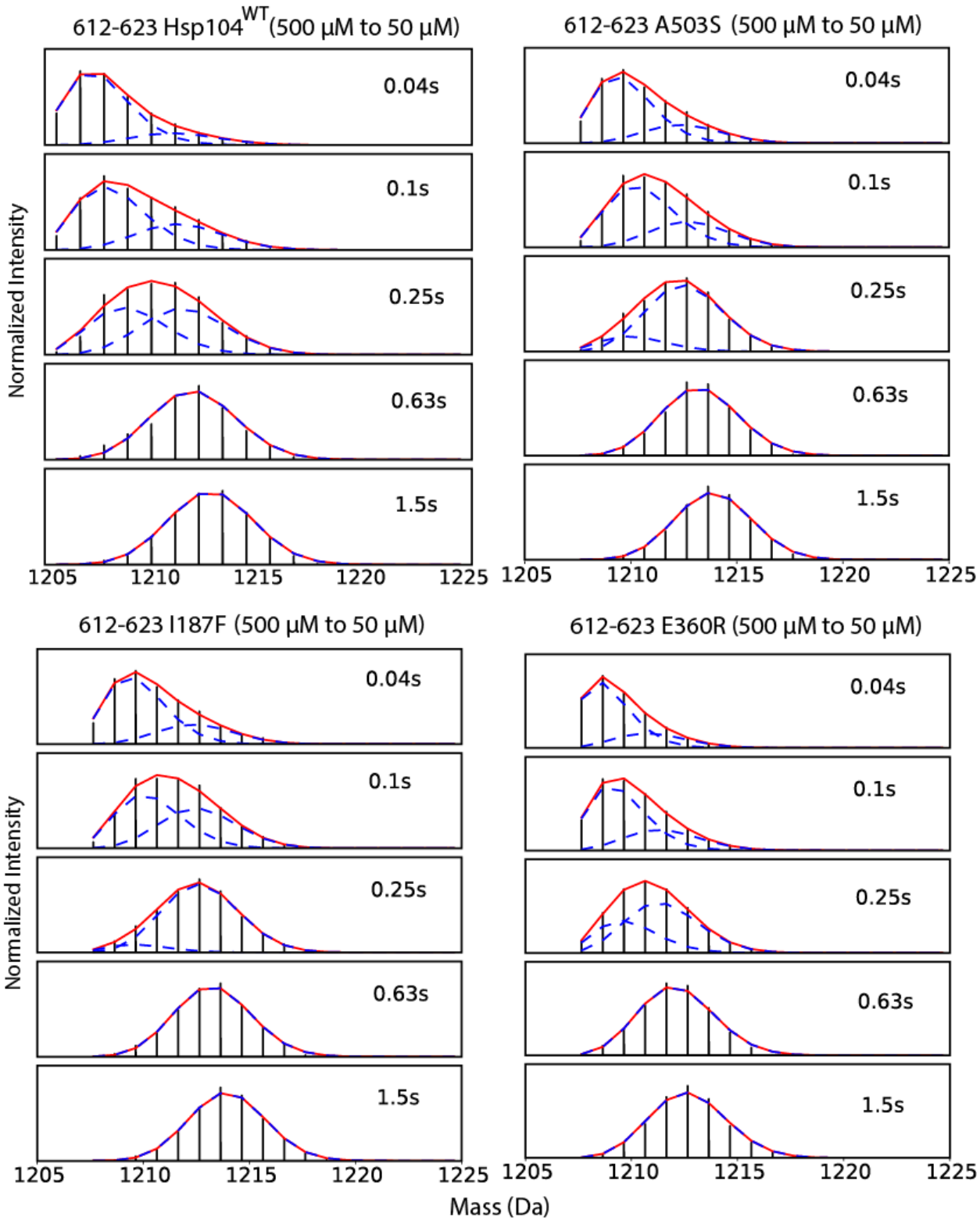

Fig. SI 4. ADP dissociation kinetics from NBD2 are not affected by the potentiating mutations. HX MS spectra of the Walker A segment in NBD2 as ADP dissociates show that WT and the potentiated mutants all display very similar spectral overlap indicating similarly fast ADP dissociation and rebinding kinetics.

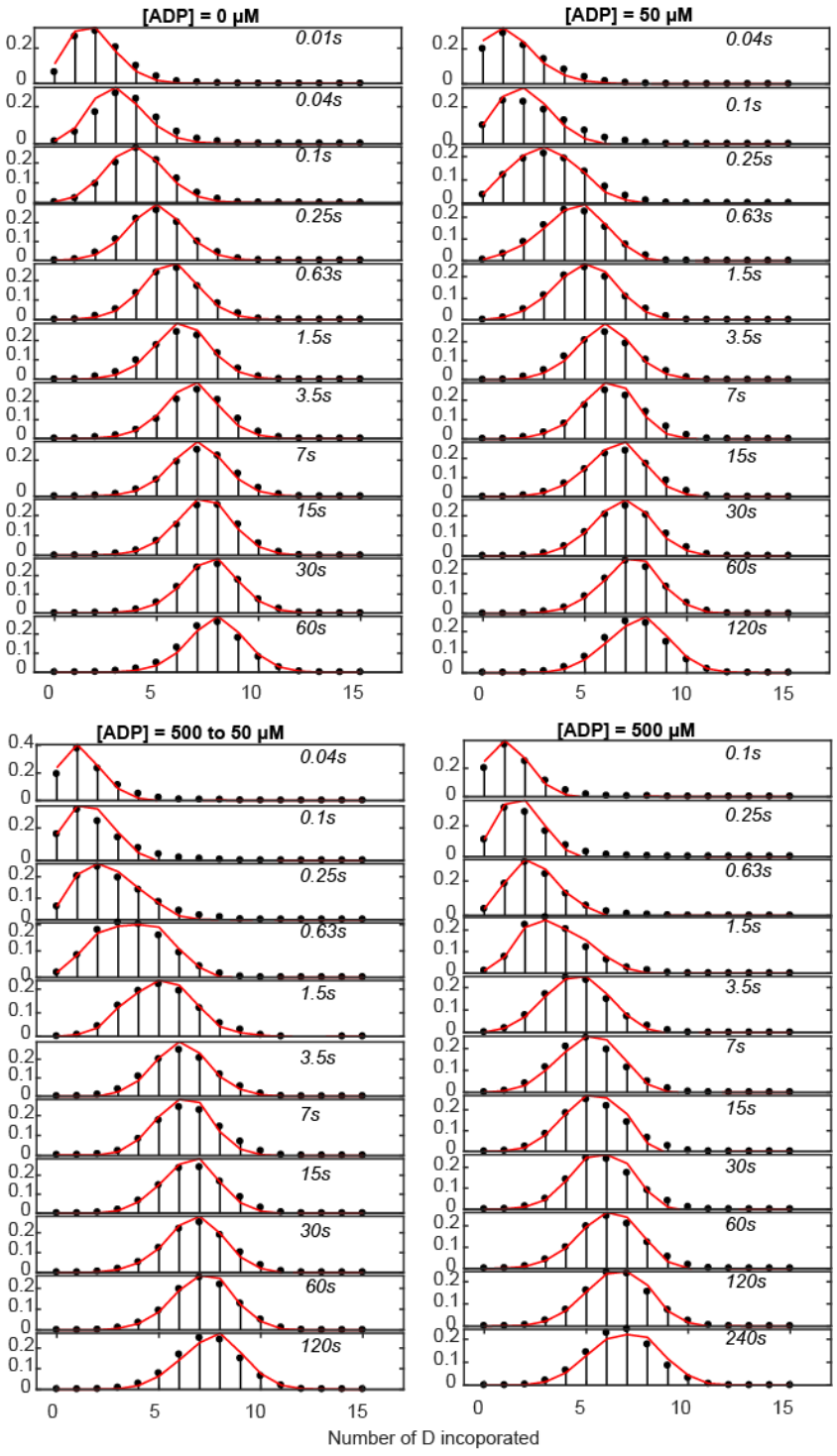

Fig. SI 5. The good quality of fit to MS spectra used to extract ADP binding kinetics at Walker A NBD2 of WT Hsp104. ADP rebinding rate was calculated by finding the best fit to the measured HX MS envelopes with Eq. 1, with floating ADP k_{on} and k_{off} and the known unbound Walker A HX rates. The black vertical lines are experimental data. The red curves are generated using the best fit parameters calculated for the competition between D-labeling and ADP rebinding as detailed in Supplementary Methods.

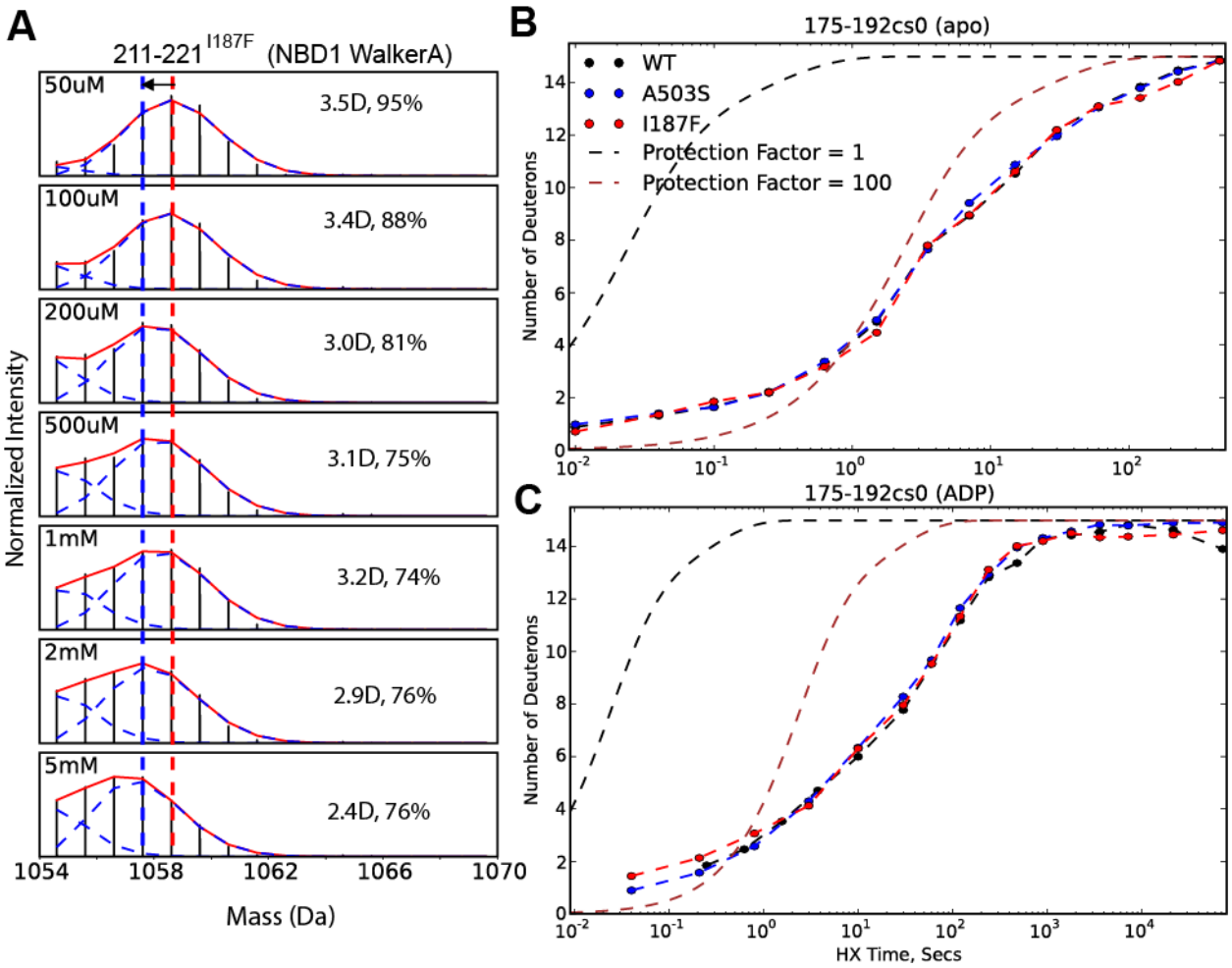

Fig. SI 6. Effects of I187F on ADP binding at NBD1 Walker A (211-221) and at the interhelical B2-B3 loop (175-192). (A) MS spectra showing heterogeneous lower and higher affinity equilibrium ADP binding to NBD1 Walker A in the I187F variant, as displayed in main text Fig. 2F. I187F Hsp104 was pre-incubated with the ADP concentration indicated, and exposed to H to D exchange for 40 ms. Two populations are distinguished by the presence or absence of HX protection due to ADP binding. A minor fraction, ~1/3, displays protection against D-labeling due to ADP binding (lighter less deuterated population) with *Kd* ~140 μM, but a larger population fraction (~2/3) of NBD1 binding sites remains unprotected (heavier more deuterated, centroids of this population in terms of number of D incorporation and percentages are labeled in the figure) indicating little ADP binding. This observation matches the two different ADP binding populations in I187F Hsp104 (main text Fig. 2F). When exposed to still higher concentrations of ADP the centroid of the low affinity population is seen to slide noticeably towards lower mass, becoming more protected as ADP begins to bind (vertical red and blue lines to guide the eye), yielding a rough estimate of ADP K_d ~2 mM for this low affinity population. **(B&C)** HX of the inter-helical B2-B3 loop shows little effect of I187F (or A503S) on this region in either the apo (B) or ADP-bound state (C). Under ATP turnover conditions, the B2 - B3 loop in I187F Hsp104 becomes significantly protected (main text Fig. 5), as does the MD L1 helix, suggesting a cross-protomer interaction in the closed state that would explain the effect of I187F on ATPase cooperativity and its promotion of the closed state.

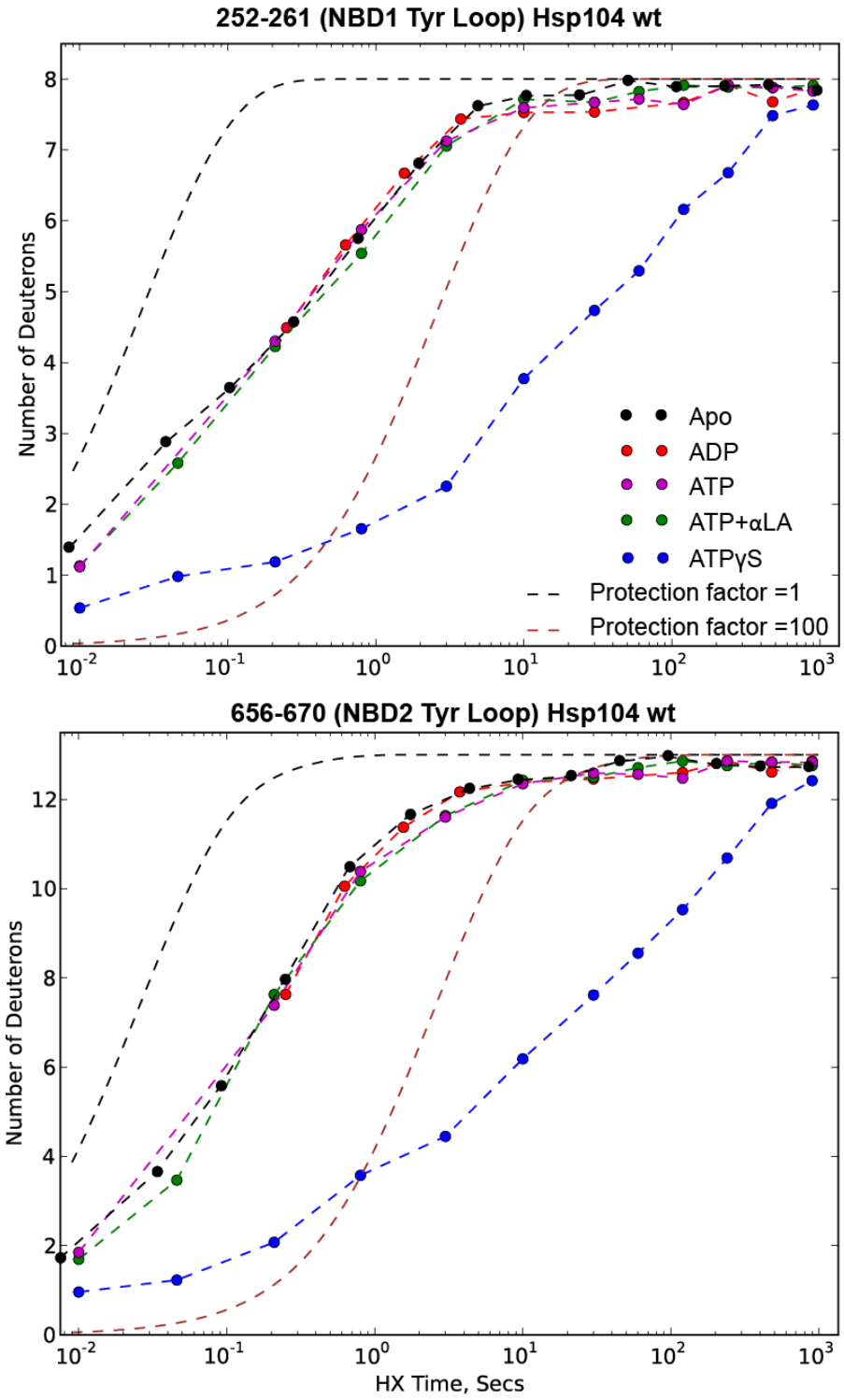

Fig. SI 7. Tyr loop HX reveals the global open/closed condition. (A) NBD1. **(B)** NBD2. The Tyr loops are flexible and fast exchanging in the open state. ATPγS binding generates the static closed state and slows HX of the Tyr loops in both NBD1 and NBD2 by 100-fold. All other states spend all or most of their time in the fast exchanging open state with low protection factor ~10.

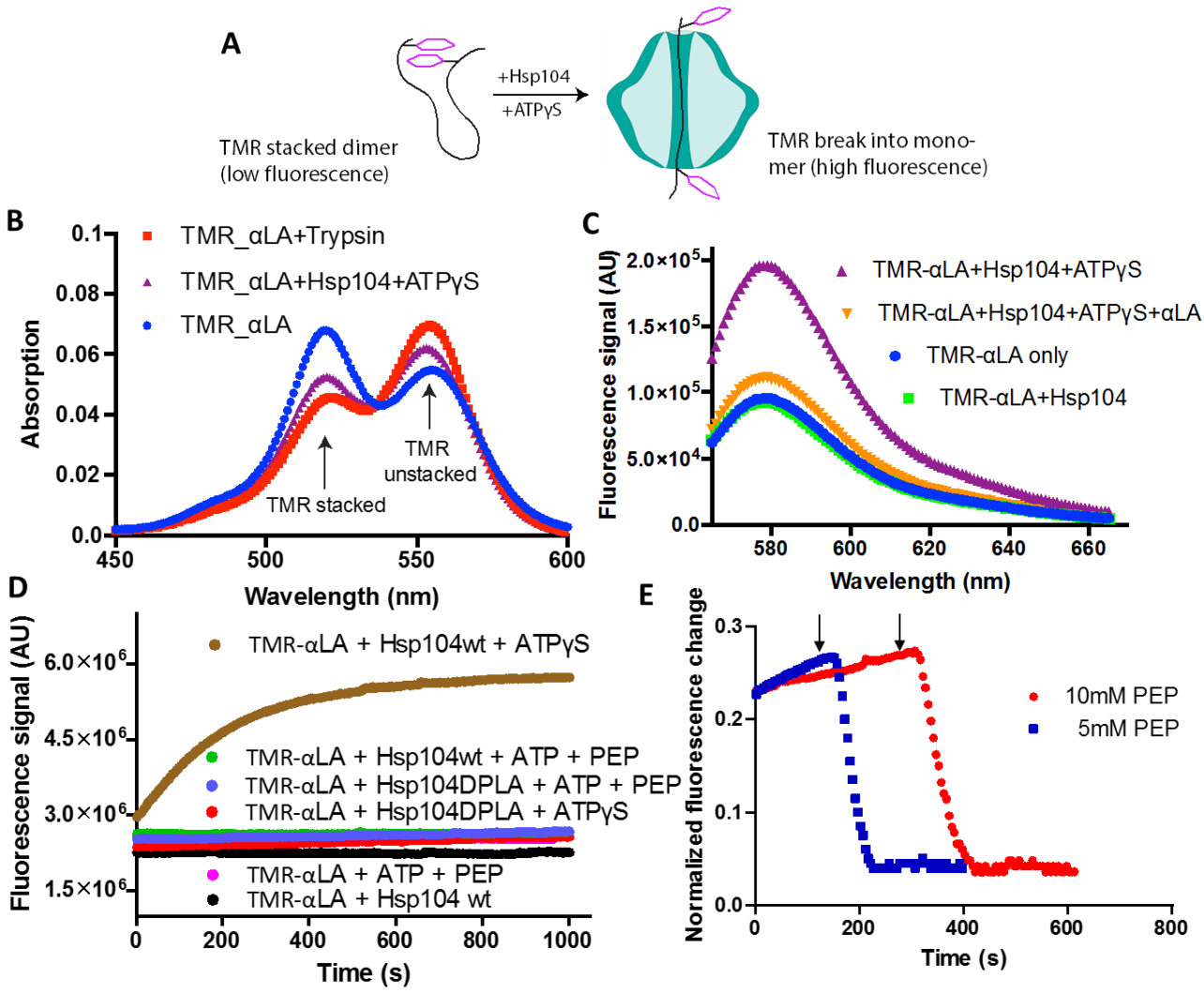

Fig. SI 8. The measurement of Hsp104 interaction with substrate protein α-lactalbumin (αLA) doubly labeled with tetramethylrhodamine (TMR). (A) Schematic illustration of doubly labeled TMR-αLA, when stacked and unstacked. **(B)** Changes in absorbance signals of TMR-αLA (500nM). In free solution the two TMR labels stack (blue). They unstack when separated by trypsin cutting (red) or when bound to closed state Hsp104 (6μM Hsp104 protomer + 5mM ATPγS; magenta), characterized by a red shift in absorbance spectrum. **(C)** Changes in TMR-αLA (300nM) fluorescence (excitation 555 nm, emission 565-665 nm) upon binding to Hsp104 (4 μM) in the presence of ATPγS (5mM). The fluorescence increase is reversed when labeled αLA is displaced by added unlabeled αLA (3 μM) (from magenta to orange). **(D)** Fluorescence change due to TMR-αLA (300nM) interacting with closed state Hsp104 induced by ATPγS binding. In other states fluorescence is low (due to absence of binding or substrate loss). The fluorescence signal reflects labeled TMR-αLA entry into and retention within the central pore, and not some non-specific interaction. This is indicated by the absence of fluorescence signal in the double pore-loop mutant (DPLA, Y257A/Y662A) and also in the open state produced in the absence of nucleotide, or during steady-state ATP turnover, or when ATP is exhausted. **(E)** TMR fluorescence due to retention of labeled αLA by I187F Hsp104 during steady state ATP turnover (normalized to high level upon ATPγS binding, as in (D)). An ATP regenerating system was used (Methods) with two different

phosphoenolpyruvate (PEP) concentrations as indicated. When PEP is exhausted (indicated by the arrows in Panel E), ADP accumulates, Hsp104 shifts to the open state, and fluorescence decays reflecting substrate release.

References

1. Sweeny EA, DeSantis ME, & Shorter J (2011) Purification of hsp104, a protein disaggregase. *J Vis Exp* (55).
2. Tariq A, Lin J, Jackrel ME, Hesketh CD*, et al.* (2019) Mining disaggregase sequence space to safely counter TDP-43, FUS, and alpha-synuclein proteotoxicity. *Cell Rep* 28(8):2080-2095 e2086.
3. Desantis ME, Sweeny EA, Snead D, Leung EH*, et al.* (2014) Conserved distal loop residues in the Hsp104 and ClpB middle domain contact nucleotide-binding domain 2 and enable Hsp70-dependent protein disaggregation. *J Biol Chem* 289(2):848-867.
4. Ye X, Lin J, Mayne L, Shorter J, & Englander SW (2019) Hydrogen exchange reveals Hsp104 architecture, structural dynamics, and energetics in physiological solution. *Proc Natl Acad Sci U S A* 116(15):7333-7342.
5. Kan ZY, Walters BT, Mayne L, & Englander SW (2013) Protein hydrogen exchange at residue resolution by proteolytic fragmentation mass spectrometry analysis. *Proc Natl Acad Sci U S A* 110(41):16438-16443.
6. Walters BT, Ricciuti A, Mayne L, & Englander SW (2012) Minimizing back exchange in the hydrogen exchange-mass spectrometry experiment. *J Am Soc Mass Spectrom* 23(12):2132-2139.
7. Mayne L, Kan ZY, Chetty PS, Ricciuti A*, et al.* (2011) Many overlapping peptides for protein hydrogen exchange experiments by the fragment separation-mass spectrometry method. *J Am Soc Mass Spectrom* 22(11):1898-1905.
8. Weaver CL, Duran EC, Mack KL, Lin J*, et al.* (2017) Avidity for polypeptide binding by nucleotide-bound Hsp104 structures. *Biochemistry* 56(15):2071-2075.
9. Ewbank JJ & Creighton TE (1993) Structural characterization of the disulfide folding intermediates of bovine alpha-lactalbumin. *Biochemistry* 32(14):3694-3707.
10. Kan ZY, Ye X, Skinner JJ, Mayne L, & Englander SW (2019) ExMS2: An integrated solution for hydrogen-deuterium exchange mass spectrometry data analysis. *Anal Chem* 91(11):7474-7481.
11. Norby JG (1988) Coupled assay of na+,k+-ATPase activity. *Methods Enzymol* 156:116-119.
12. Kuwajima K, Ikeguchi M, Sugawara T, Hiraoka Y, & Sugai S (1990) Kinetics of disulfide bond reduction in alpha-lactalbumin by dithiothreitol and molecular basis of superreactivity of the cys6-cys120 disulfide bond. *Biochemistry* 29(36):8240-8249.

SUPPLEMENTARY INFORMATION APPENDIX
TOTAL COLLECTION OF MASS CENTROID PLOTS FOR APO, ADP, ATP HSP104

A list of critical Hsp104 structural motifs or domains:

Walker A: 212-219 (NBD1), 614-621 (NBD2)

Walker B: 279-285 (NBD1), 682-687 (NBD2)

Sensor 1: T317 (NBD1), N728 (NBD2)

Sensor 2: R826 (NBD2)

Arg finger: R333/334 (NBD1), R765 (NBD2)

Tyr loop: 251-259 (NBD1), 659-666 (NBD2)

NTD: 1-164

NBD1: 165-411 & 538-556, including small domain (345-411 & 538-556)

MD: 412-537, including L1 (413-433), L2 (439-496), L3 (498-505), L4 (510-525)

NBD2: 557-870

CTD: 871-908